

Research Article

An Investigation of Palladium Oxygen Reduction Catalysts for the Direct Methanol Fuel Cell

G. F. Álvarez, M. Mamlouk, and K. Scott

School of Chemical Engineering and Advanced Materials, Newcastle University, Newcastle upon Tyne NE1 7RU, UK

Correspondence should be addressed to M. Mamlouk, mohamed.mamlouk@ncl.ac.uk

Received 28 September 2010; Revised 6 December 2010; Accepted 14 December 2010

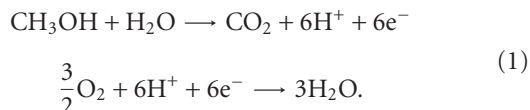
Academic Editor: Jiujuan Zhang

Copyright © 2011 G. F. Álvarez et al. This is an open access article distributed under the Creative Commons Attribution License, which permits unrestricted use, distribution, and reproduction in any medium, provided the original work is properly cited.

A comparative study of Pd and Pt was carried out in DMFC using different methanol concentrations and under different operating conditions. Cell performance was compared at methanol concentrations of 1, 3, 5, and 7 M and at temperatures of 20, 40, and 60°C. Homemade Pd nanoparticles were prepared on Vulcan XC-72R using ethylene glycol as the reducing agent at pH 11. The resulting catalyst, Pd/C, with metal nanoparticles of approximately 6 nm diameter, was tested as a cathode catalyst in DMFC. At methanol concentrations of 5 M and higher, the Pd cathode-based cell performed better than that with Pt at 60°C with air.

1. Introduction

Among liquid organic fuels methanol is a good candidate for direct electrochemical oxidation in terms of reactivity at low temperatures, handling, and storage. Methanol-fed polymer electrolyte membrane fuel cells would be convenient because this would avoid many difficulties encountered when operating with hydrogen-fed fuel cells, such as gas storage and reforming. In a direct methanol fuel cell (DMFC), methanol is oxidized to carbon dioxide in the anode and protons cross the electrolyte membrane and combine with oxygen at the cathode to form water. Equation (1) describe anodic and cathodic reactions occurring in a polymer acid electrolyte DMFC:



One of the major technical problems of current DMFCs is the methanol crossover, that is, methanol permeation from the anode compartment through the electrolyte membrane to the cathode compartment. This causes cathode performance losses due to the formation of mixed potentials on the cathode catalyst as well as the decrease in the efficiency of methanol utilization [1]. To avoid mixed potentials in the cathode, caused by the simultaneous methanol oxidation and

oxygen reduction reactions taking place, a possible solution would be employing a cathode electrocatalyst selective for the ORR.

Previous studies showed that Ru-based catalysts (e.g., Ru-Se, Ru-Se-Mo, and Ru-Se-Rh) have some promising properties, that is, reasonably high activity for oxygen reduction and high methanol tolerance [2–4]. Another possible candidate to substitute Pt is Pd. Palladium, like platinum, has a four-electron pathway for the oxygen reduction reaction and its activity for ORR is only surpassed by platinum [5]. Additionally, Pd has negligible electrocatalytic activity towards methanol oxidation in acid medium [6].

Lee et al. studied the ORR in acid media in the presence of methanol on Pt, Pd, and Pd alloys [6]. They found that the Pt electrode exhibited a large anodic current above ca. 0.75 V versus NHE due to methanol oxidation. This methanol oxidation led to an onset potential ca. 200 mV lower than that observed without methanol in the electrolyte, which was attributed to the formation of a mixed potential on the Pt surface. Pd and Pd alloy electrocatalysts did not show mixed potential in the presence of both oxygen and methanol. Several groups have reported enhanced activity of Pd-Pt catalyst towards selective ORR compared to pure Pt in the presence of methanol [7–9].

Optimized carbon-supported palladium catalyst, Pd/C, was considered as a candidate cathode catalyst because of its

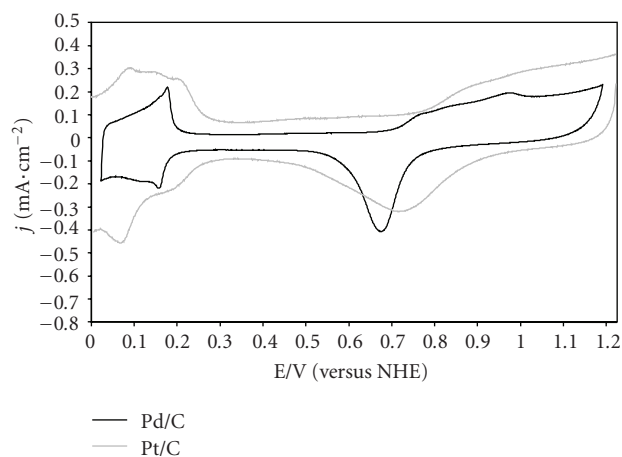


FIGURE 1: Comparison of cyclic voltammograms of Pd/C and Pt/C in N_2 saturated $0.5 M H_2SO_4$ solution at room temperature, scan rate $5 mV s^{-1}$.

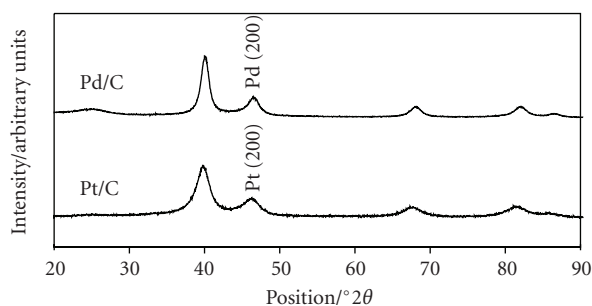


FIGURE 2: XRD patterns of carbon-supported palladium and platinum catalysts.

high activity towards oxygen reduction in a direct methanol fuel cell. Cell performance with Pd/C in the cathode was compared with the performance when using commercial Pt/C as cathode catalyst. Cell potentials at low current densities were compared ($5 mA \cdot cm^{-2}$) and current densities at $400 mV$ were chosen for the purpose. A constant methanol flow rate of $7 mL \cdot min^{-1}$ was used in every test; this flow rate was chosen for being the optimum for $1 M$ methanol according to studies published by Lin et al. [10].

The effect of methanol concentration on cell performance was studied using methanol solutions of 1 to $7 M$. Temperature was studied in the range of 20 , 40 , and $60^\circ C$.

2. Experimental

Electrochemical surface area (ECSA) of the electrocatalysts was quantified from slow scan voltammograms, at scan rate $5 mV s^{-1}$, using a rotating disc electrode in oxygen free $0.5 M H_2SO_4$ solution. The electrode was previously conditioned by undergoing cycles at scan rate of $50 mV s^{-1}$; after this conditioning slow voltammograms were recorded. Potential range at which the electrode was cycled at scan rate $5 mV s^{-1}$.

X-ray diffraction analyses were carried out using a PAN analytical X'Pert Pro diffractometer fitted with an X'Celerator and peak positions were analysed using the X'Pert Data Viewer software. The radiation was Cu K-alpha, with $\lambda = 1.54180 \text{ \AA}$. Analyses were performed by the Chemical Analysis Unit at Newcastle University.

Membrane electrode assemblies (MEAs) were prepared by hot pressing a membrane and electrodes at $130^\circ C$ for $3 min$, applying a load of ca. $50 kg \cdot cm^{-2}$. Nafion 117 was used as the electrolyte membrane; the received material was boiled in 2% hydrogen peroxide for $30 min$, rinsed with deionized water, and then boiled with $1 M H_2SO_4$ for $1 hour$ before being thoroughly washed with deionized water. The electrodes were prepared as follows using catalysts inks. Metal loadings were $2 mg \cdot cm^{-2}$ PtRu in the anode and $2 mg \cdot cm^{-2}$ of Pd or Pt in the cathode. Catalysts used were commercial carbon-supported PtRu 60% weight (E-Tek) for the anode and commercial carbon-supported Pt 20% weight (E-Tek) or in house made Pd/C 20% weight. In the preparation of Pd/C, $40 cm^3$ (mL) of ethylene glycol (Aldrich, 99.8%) were mixed with $0.300 g$ of Vulcan XC-72R under magnetic stirring and nitrogen flow. The pH of the solution was adjusted with drops of $1 M NaOH$ (Aldrich, 98%) solution. $20 cm^3$ of an aqueous solution containing $0.203 g$ of $(NH_4)_2PdCl_4$ (Aldrich, 99.995%) were added dropwise whilst maintaining the pH constant. The mixture was heated to $110^\circ C$ and refluxed for $3 hours$. The catalyst was thoroughly washed with deionised water and acetone and dried overnight under air at $100^\circ C$.

The catalyst ink was prepared by mixing in an ultrasonic bath the carbon-supported catalyst with a water:ethanol mixture with Nafion solution for $30 min$. The amount of Nafion in the catalyst ink was 15% of the catalyst weight. Catalyst layers were sprayed on a commercial wet proofed gas diffusion layer, (CX196, from Freudenberg, Germany).

The fuel cell body was made of two graphite blocks each with $3 cm \times 3 cm$ parallel flow fields. The temperature of the cell was controlled by heating pads located at both sides of the cell body. Operating temperatures were 20 , 40 , and $60^\circ C$. Aqueous $1 mol \cdot dm^{-3}$ (M) methanol solution was pumped into the anode at a rate of ca. $7 mL \cdot min^{-1}$ using a Watson Marlow 101 U/R pump. Air or oxygen was fed to the cathode side at a rate of approximately $300 mL \cdot min^{-1}$. Gas flow rate was controlled manually by appropriate flow meters (Platon (RM&C), U.K) and was fed at atmospheric pressure.

Immediately before recording polarisation data reported in this piece of work, each MEA was conditioned by undergoing ten potential cycles at scan rate $50 mV s^{-1}$ between OCP and $0 V$; after this scan rate, $2 mV s^{-1}$ was used until reproducible I-V curve was obtained; the reproducible curve was then finally recorded.

3. Results and Discussion

Catalysts compared in this study were homemade Pd nanoparticles (Pd/C) and commercial Pt catalyst (Pt/C); both were electrochemically characterized by cyclic voltammetry using a rotating disc electrode in oxygen free

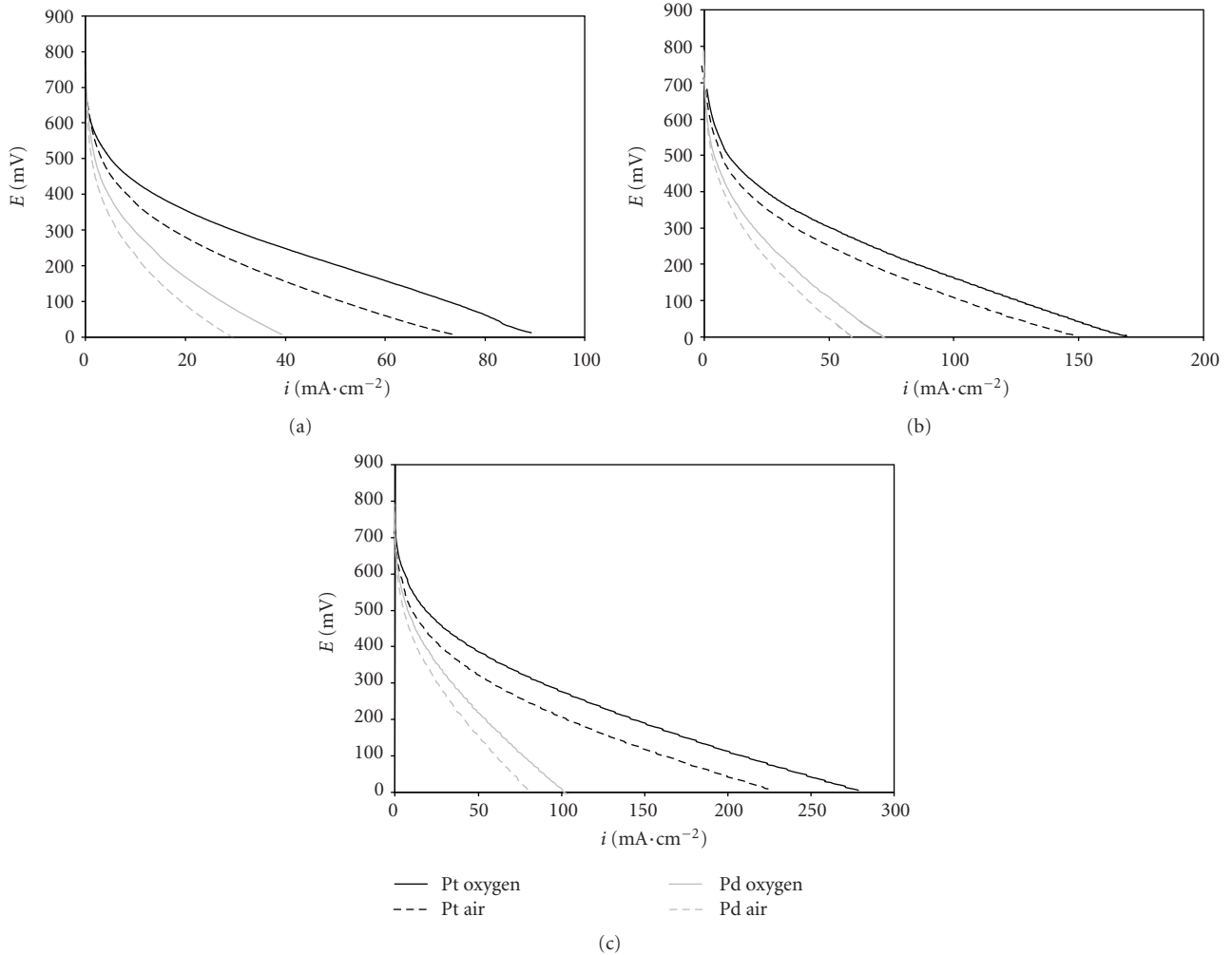


FIGURE 3: (a) Comparison of polarization curves of a direct methanol fuel cell with Pd/C and commercial Pt/C from E-tek as cathode catalyst at 20°C and 1 M methanol. (b) Comparison of polarization curves of a direct methanol fuel cell with Pd/C and commercial Pt/C from E-tek as cathode catalyst at 40°C and 1 M methanol. (c) Comparison of polarization curves of a direct methanol fuel cell with Pd/C and commercial Pt/C from E-tek as cathode catalyst at 60°C and 1 M methanol.

0.5 M H_2SO_4 solution [11]. Figure 1 compares slow scan cyclic voltammograms for Pd/C and Pt/C.

For palladium electrodes, in contrast with platinum, the charge of a monolayer of adsorbed hydrogen is difficult to determine due to the ability of bulk palladium to absorb hydrogen [12, 13]. Therefore, the electrochemical surface area was calculated from the charge of the monolayer of chemisorbed oxygen, which was estimated from the area of the palladium oxide reduction peak. The charge of the oxygen monolayer (Q_{O}) for a smooth palladium electrode is twice as large as the hydrogen monolayer (Q_{H}) in platinum, $Q_{\text{H}} = 1/2 Q_{\text{O}}$ ($Q_{\text{H}} = 210 \mu\text{C cm}^{-2}$) [12]. ECSA values for both electrocatalysts are shown in Table 1.

Figure 2 shows XRD patterns corresponding to carbon-supported platinum and palladium catalysts. A broad peak at a 2θ value around 25° , due to the carbon support [14], was present in every spectrum. Data from diffraction peaks corresponding to Pd (220) and a Pt (220) crystal faces, which were considered not to be influenced by the presence

TABLE 1: ECSA and particle size for carbon-supported palladium catalysts.

Catalyst	Particle size (nm)	ECSA ($\text{m}^2 \text{g}^{-1}$)
Pd/C	7.3	14.6
Pt/C	3.4	55.3

of carbon, were employed in calculations [15, 16]. The crystallite size, referred to as particle size, was calculated from the XRD data using Scherrer equation [17]:

$$D = k \times \frac{\lambda}{FWHM} \times \cos \theta. \quad (2)$$

Particle sizes estimated using Scherrer equation are shown in Table 1.

3.1. Effect of Methanol Concentration on Fuel Cell Performance. Li et al. [18] compared ORR activity of Pd/C and

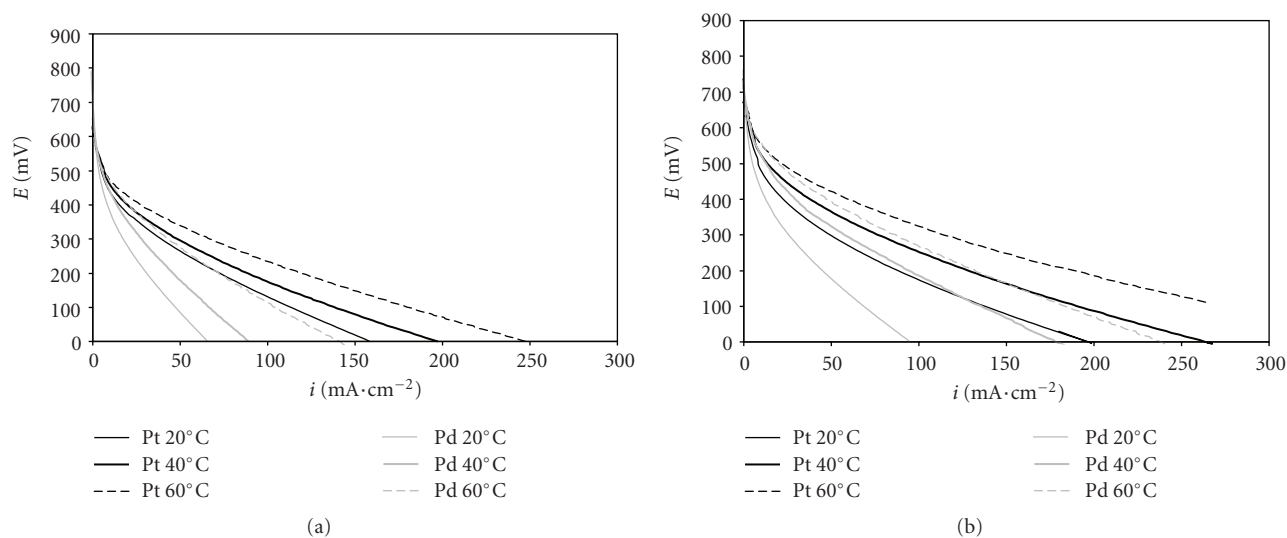


FIGURE 4: (a) Comparison of polarization curves of a direct methanol fuel cell operating with air and 3 M methanol with Pd/C and commercial Pt/C from E-tek as cathode catalyst at 20, 40, and 60°C. (b) Comparison of polarization curves of a direct methanol fuel cell operating on oxygen and 3 M methanol with Pd/C and commercial Pt/C from E-tek as cathode catalyst at 20, 40, and 60°C.

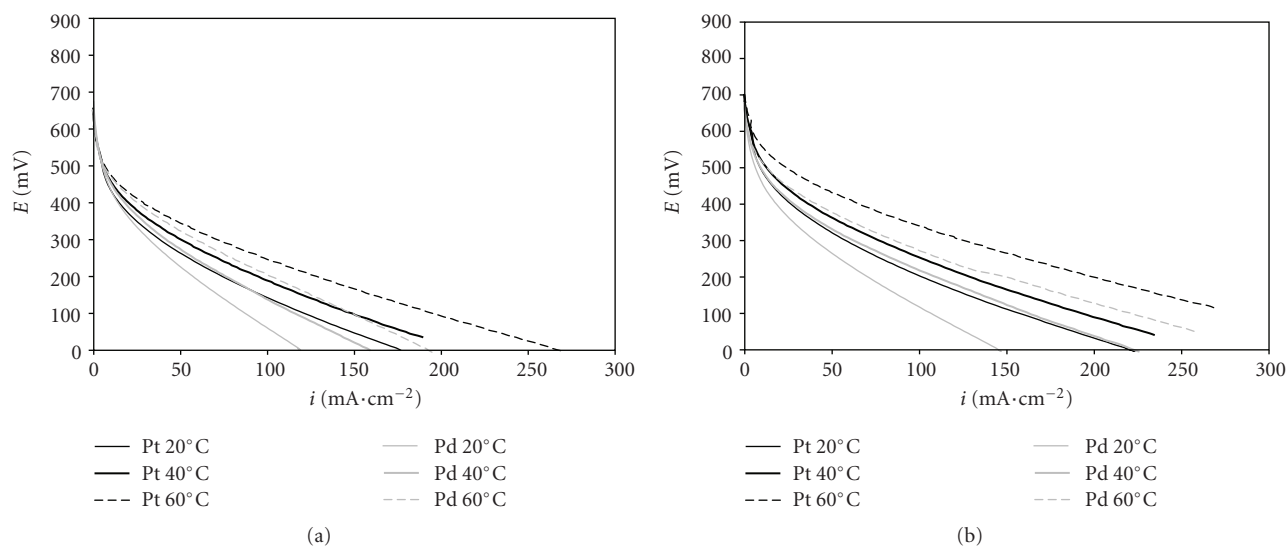


FIGURE 5: Comparison of polarization curves of a direct methanol fuel cell operating with air and 5 M methanol with Pd/C and commercial Pt/C from E-tek as cathode catalyst at 20, 40, and 60°C.

$\text{Pd}_4\text{Co}_1/\text{C}$ with that of Pt/C, with and without methanol in the electrolyte. They found that although Pt/C presents superior ORR performance than Pd/C and $\text{Pd}_4\text{Co}_1/\text{C}$ in pure 0.5 M HClO_4 electrolyte, in the methanol containing solution, ORR activity of Pt/C was much lower, while that of Pd/C and $\text{Pd}_4\text{Co}_1/\text{C}$ was stable.

Measured exchange current densities at room temperature for the oxygen reduction reaction (ORR) on platinum and palladium electrodes were 1.4×10^{-10} and $7.7 \times 10^{-12} \text{ A} \cdot \text{cm}_{\text{metal}}^{-2}$ [11]. Considering the activation energy of the oxygen reduction reaction on Pd/C, ca. 90 kJ mol^{-1} [19], and on Pt/C, ca. 26 kJ mol^{-1} [20], the exchange current density for ORR at 50°C on platinum can be estimated to be 3.2×10^{-10} in comparison to $1.3 \times 10^{-10} \text{ A} \cdot \text{cm}_{\text{ESA}}^{-2}$ for

palladium. In other words, at 50°C platinum is 2.5 times more active than palladium for ORR. On the other hand, the exchange current density for the methanol oxidation reaction (MOR) at 50°C is reported [21] to be ca. $3 \times 10^{-8} \text{ A} \cdot \text{cm}_{\text{metal}}^{-2}$ on platinum and ca. $10^{-11} \text{ A} \cdot \text{cm}_{\text{metal}}^{-2}$ on palladium. This means at 50°C platinum is approximately 3000 times more active than palladium for the methanol oxidation reaction. Calculating the ratio of $i_{0(\text{MOR})}/i_{0(\text{ORR})}$ for both catalyst at 50°C, we obtain ca. 100 and 0.1 for Pt and Pd, respectively. This suggests that platinum is approximately 100 times more active (more selective) for methanol oxidation than for oxygen reduction, and therefore the effects of any crossed-over methanol would be severe. On the contrary, palladium is approximately 10 times less active for MOR in comparison

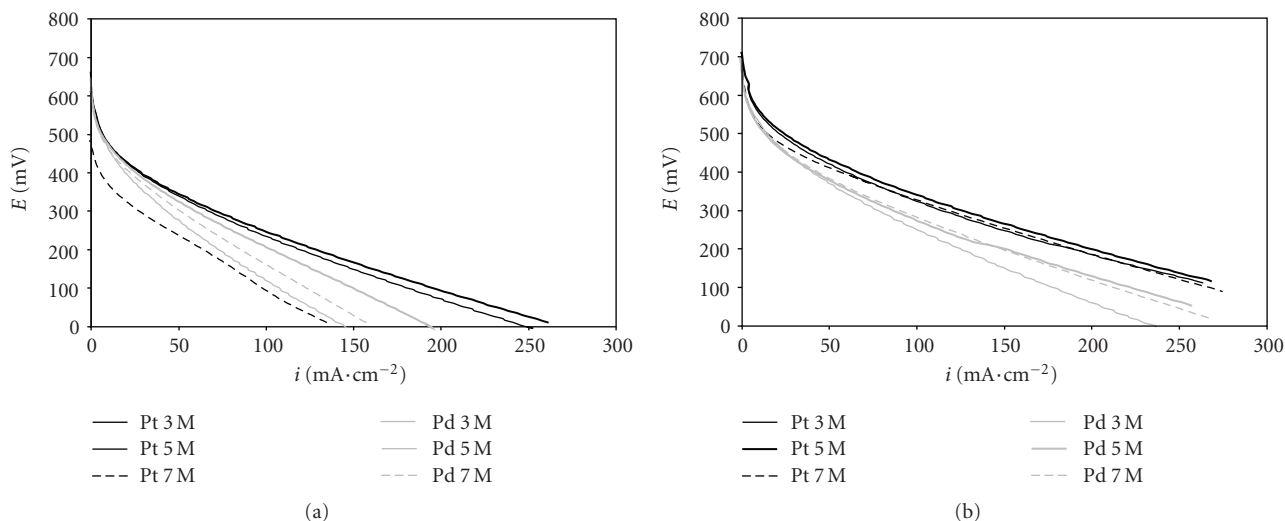


FIGURE 6: (a) Comparison of polarization curves of a direct methanol fuel cell operating with air with Pd/C and commercial Pt/C from E-tek as cathode catalyst at 60°C and 3, 5, and 7 M methanol. (b) Comparison of polarization curves of a direct methanol fuel cell operating with oxygen with Pd/C and commercial Pt/C from E-tek as cathode catalyst at 60°C and 3, 5, and 7 M methanol.

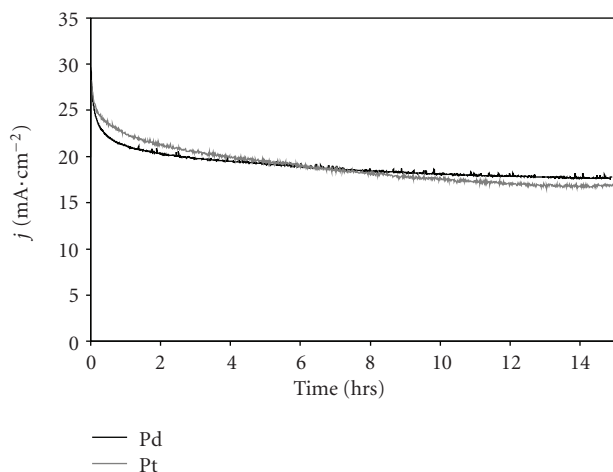


FIGURE 7: Chronoamperometry measurements of DMFC with Pd/C or Pt/C as cathode catalyst using the same anode materials (Pt-Ru/C) at 20°C and 5 M methanol, with oxygen.

to ORR, thus palladium is a more selective catalyst for ORR than MOR. Therefore, it can be concluded that palladium is a good candidate for methanol fuel cell cathodes (DMFCs) especially at higher methanol concentration and higher operating temperatures.

3.1.1. Cell Polarizations. Figure 3 compares potential-current curves for the palladium electrocatalyst and commercial Pt/C cathode materials using 1 M methanol at 20, 40, and 60°C , operating with air and oxygen.

The open circuit potentials of palladium were ca. 30 mV higher than that of Pt at 20°C ; however, as temperature increases similar OCP was observed for both catalysts when using 1 M methanol at the anode. However, the ORR

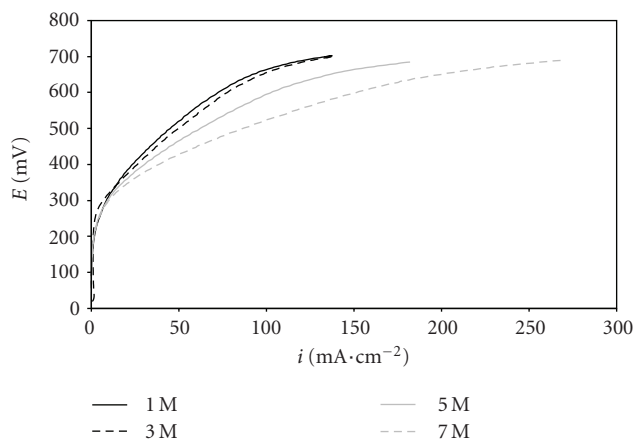


FIGURE 8: Anode polarization curves for a fuel cell with PtRu/C from E-tek anode catalyst and Pd/C cathode catalyst at 60°C fed with methanol 1, 3, 5, and 7 M with air operation.

kinetics on Pd cathodes was sluggish in comparison to Pt, demonstrated by larger activation losses in the kinetic region.

Cell voltages in different conditions, summarised in Table 2, were larger for the Pt MEA in every case. The difference in cell voltage between Pt and Pd MEAs was similar when the cell was operating with air or oxygen. For example, at 20°C and at $5\text{ mA}\cdot\text{cm}^{-2}$ the difference was 116 mV for air and 107 mV for oxygen, decreasing to 88 mV for air and 81 mV for oxygen at 40°C and 67 mV for air and 63 mV for oxygen at 60°C . This tendency was also observed at higher current densities; comparing cell potentials at $20\text{ mA}\cdot\text{cm}^{-2}$, at 20°C , the difference between Pt and Pd was 188 mV for air and 187 mV for oxygen, decreasing to 124 mV for air, both air and oxygen at 40°C , 95 mV for air, and 101 mV for oxygen at 60°C . The decreasing difference with increasing

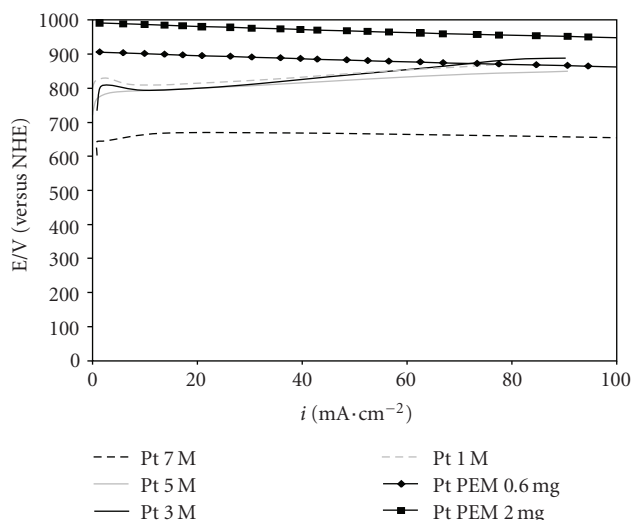


FIGURE 9: Cathode polarization curves for Pt MEA for a DMFC at 60°C fed with 1, 3, 5, and 7 M methanol solution with air operation compared to experimental (0.6 mg) and predicted (2.0 mg) data from a H₂ PEM fuel cell

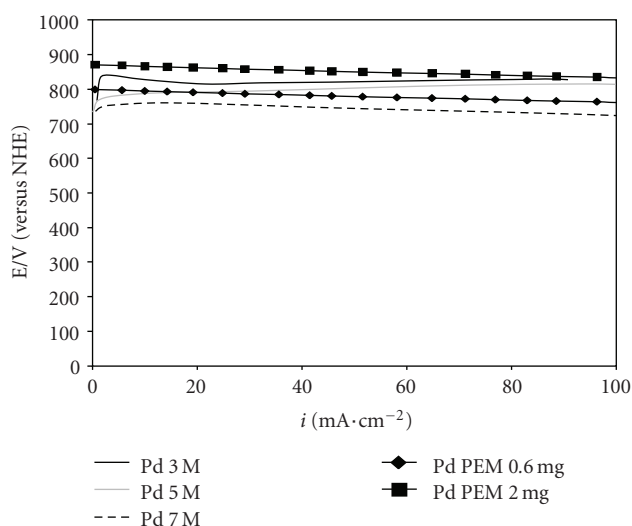


FIGURE 10: Cathode polarization curves for Pd MEA for a DMFC at 60°C fed with 3, 5, and 7 M methanol solution compared to data from a H₂ PEM fuel cell.

temperature between Pd and Pt cell potentials at low current densities would indicate that the activation energy of the oxygen reduction reaction on Pd is higher than on Pt, which was already shown for hydrogen PEM fuel cells [11].

The effect of air or oxygen on cell voltage for a given operating current density depended on oxygen mass transport in the cathode and methanol crossover effects. The methanol crossover effect will be more pronounced at lower oxygen concentration.

No reports for pure Pd cathodes in direct methanol fuel cells were found in the literature; however, some palladium alloys have been tested as cathode materials in DMFC. Mustain et al. tested a DMFC with a Pd₃Co cathode and Pt anode

at 60°C operating with oxygen and 0.5 M methanol solution [22]. They observed current densities of ca. 20 mA·cm⁻² in these conditions, close to the 18 mA·cm⁻² exhibited with Pd/C with 1 M methanol obtained in our DMFC.

Figures 4(a) and 4(b) show cell polarization curves for a DMFC with Pd and Pt cathode catalysts fed with 3 M methanol solution, operating with air and oxygen, respectively.

The performance with Pd as with Pt cathodes improved significantly with an increase in temperature. The performance of the Pd MEA improved more with a temperature increase than did Pt when operating with air or oxygen due to combined effect of activation and higher methanol tolerance (methanol permeability increases with temperature).

Table 3 summarizes current densities at 0.4 V and cell voltage at 5 mA·cm⁻² for the polarization curves in Figure 2. Cell voltages at 5 mA·cm⁻² were larger for the Pt MEA in every case; however, the difference between Pd and Pt performance decreased compared to that using 1 M methanol solution. Using 3 M methanol solution, the difference in cell voltage between Pt and Pd MEAs was smaller with air operation, whilst no differences between air and oxygen were observed when the cell was operating with 1 M methanol. For example, with 3 M methanol solution at 20°C the difference was 35 mV for air and 75 mV for oxygen whilst at 60°C it was only 12 mV for air and 24 mV for oxygen. This decreased potential difference between Pd- and Pt-based DMFCs at low current densities, compared to that with 1 M methanol, would indicate that the higher methanol concentration had a more negative effect on the Pt cathode performance (higher concentration causes higher crossover rate) than on Pd. At high current densities, differences between Pd and Pt increased due to the improvement in the Pt cathode performance caused by the consumption of the crossed-over methanol when the cell was polarized [23].

Figure 5 shows polarization curves for a DMFC with Pd and Pt cathode catalysts fed with 5 M methanol solution, operating with air and oxygen, respectively. With 5 M methanol, the advantage of using Pd instead of Pt in the cathode, with lower activity towards the methanol oxidation reaction, became evident. The open circuit potential becomes higher for Pd-based cathodes than that of Pt (using 5 M methanol) at 20°C with air operation and similar to that of Pt with oxygen operation (Table 4). This is because the OCP of MEA with Pt cathode dropped by 56 mV (air, 20°C) in comparison to 11 mV for that of Pd-based cathode when methanol feed at the anode increased 5 M from to 3 M.

At low current densities (Table 4) with 5 M methanol, the palladium MEA exhibited slightly enhanced performance with increasing temperature with both oxygen and air, as expected. At 5 mA·cm⁻² with air operation at 20, 40, and 60°C, cell potentials for the Pd MEA were nearly identical to those obtained with the Pt MEA. However, with oxygen operation Pt exhibited slightly higher cell potentials than Pd at 20, 40, and 60°C (42, 26 and 29 mV). On the other hand, at larger current densities, (>ca. 20 mA·cm⁻²) the Pt MEA also showed improved performance with increased temperature similar to that obtained with 3 M methanol, due to a reduced impact of methanol crossover.

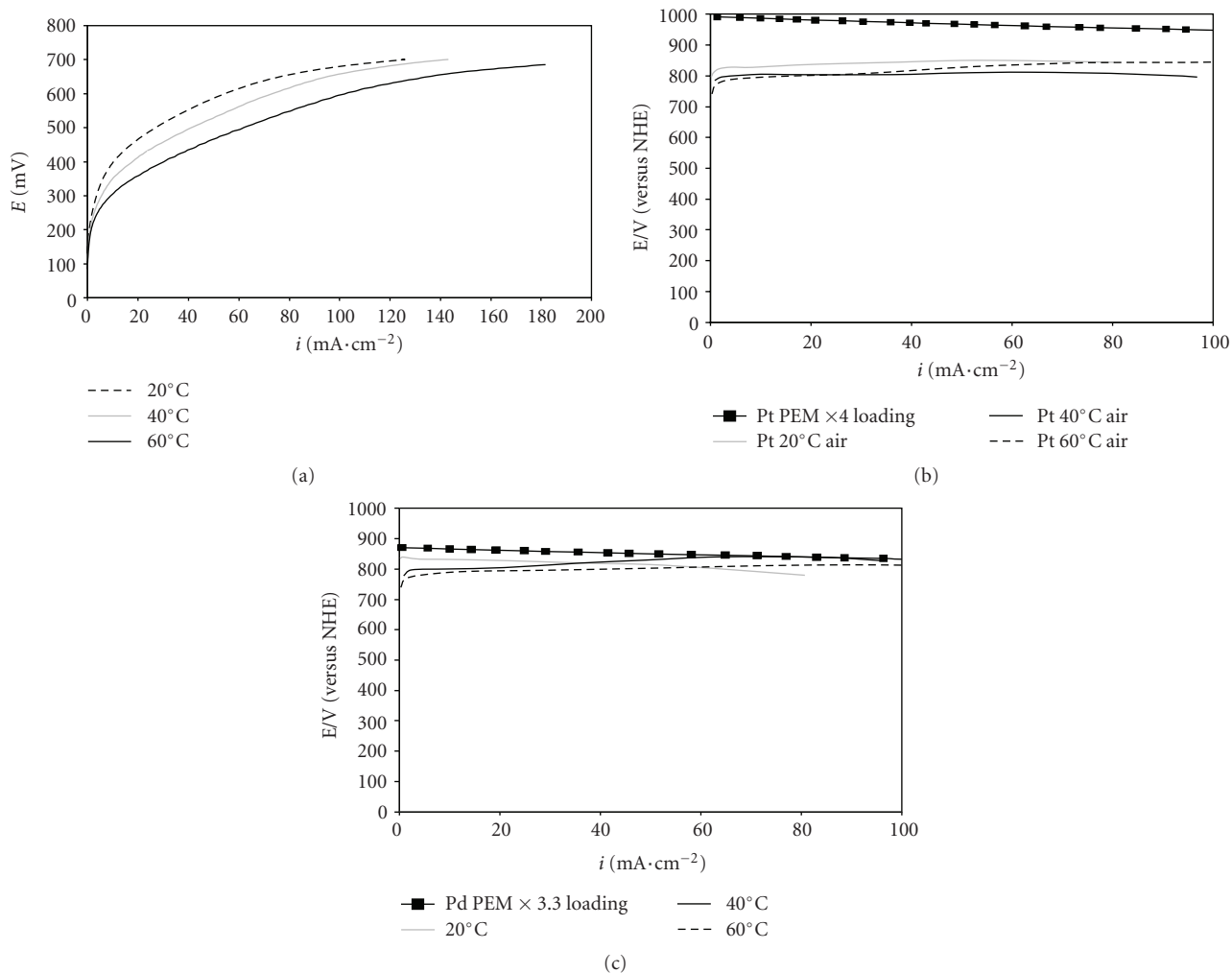


FIGURE 11: (a) Anode polarization curves for a fuel cell with PtRu/C from E-tek anode catalyst and Pd/C cathode catalyst at 20, 40, and 60°C fed with methanol 5 M. (b) Cathode polarization curves for Pt MEA for a DMFC at 20, 40, and 60°C fed with 5 M methanol solution compared to data from a H₂ PEM fuel cell. (c) Cathode polarization curves for Pd MEA for a DMFC at 20, 40, and 60°C fed with 5 M methanol solution compared to data from a H₂ PEM fuel cell.

TABLE 2: Current densities at 0.4 V, cell voltage at 5 mA·cm⁻², open circuit potential and peak power densities for a direct methanol fuel cell with 1 M methanol.

Cathode catalyst	Temperature (°C)	Cathode fed	Voltage at 5 mA·cm ⁻² (mV)	Open circuit potential (mV)	Current density at 0.4 V (mA·cm ⁻²)	Peak power density (mW cm ⁻²)
Pd/C	20	Air	335	714	3.0	2.3
Pt/C-Etek	20	Air	451	685	8.2	6.4
Pd/C	20	O ₂	390	739	4.5	3.4
Pt/C-Etek	20	O ₂	497	689	13.8	10.0
Pd/C	40	Air	448	698	7.6	5.4
Pt/C-Etek	40	Air	536	695	16.8	13.2
Pd/C	40	O ₂	482	720	10.0	6.9
Pt/C-Etek	40	O ₂	563	731	25.5	17.0
Pd/C	60	Air	500	693	12.8	8.3
Pt/C-Etek	60	Air	567	693	27.0	20.6
Pd/C	60	O ₂	542	708	18.4	11.1
Pt/C-Etek	60	O ₂	605	729	45.6	29.1

TABLE 3: Current densities at 0.4 V, cell voltage at $5 \text{ mA}\cdot\text{cm}^{-2}$, open circuit potential and peak power densities for a direct methanol fuel cell with 3 M methanol solution fed to the anode at 20, 40, and 60°C .

Cathode catalyst	Temperature ($^\circ\text{C}$)	Cathode fed	Voltage at $5 \text{ mA}\cdot\text{cm}^{-2}$ (mV)	Open circuit potential (mV)	Current density at 0.4 V ($\text{mA}\cdot\text{cm}^{-2}$)	Peak power density ($\text{mW}\cdot\text{cm}^{-2}$)
Pd/C	20	Air	455	696	8.7	6.2
Pt/C-Etek	20	Air	490	697	14.8	14.2
Pd/C	20	O_2	472	710	9.4	6.9
Pt/C-Etek	20	O_2	547	732	22.2	17.6
Pd/C	40	Air	485	680	11.5	9.3
Pt/C-Etek	40	Air	514	721	23	26.6
Pd/C	40	O_2	503	704	14.5	10.3
Pt/C-Etek	40	O_2	590	675	38	25.8
Pd/C	60	Air	507	654	16.7	19.1
Pt/C-Etek	60	Air	519	615	26.4	25.7
Pd/C	60	O_2	566	690	40	26
Pt/C-Etek	60	O_2	590	699	59.4	37.8

At 60°C and with air, the current density using Pt in the cathode decreased from 26 to $20 \text{ mA}\cdot\text{cm}^{-2}$ when methanol concentration was increased from 3 to 5 M. The opposite effect was exhibited by the MEA with Pd in the cathode, where the performance improved from 17 to $25 \text{ mA}\cdot\text{cm}^{-2}$.

Figure 6 compares polarization curves of Pd and Pt MEAs at 60°C using methanol concentrations of 3, 5, and 7 M using air and oxygen, respectively. With air, platinum cathode exhibited a small decrease in current density when changing from methanol 1 M to 3 M to 5 M (from 27 to $26 \text{ mA}\cdot\text{cm}^{-2}$ at 400 mV) and its performance fell sharply with a concentration of 7 M, to $5 \text{ mA}\cdot\text{cm}^{-2}$. However, when the platinum MEA was operated with oxygen, the effect of high methanol concentrations up to 7 M was less dramatic than with air (from 65 to $50 \text{ mA}\cdot\text{cm}^{-2}$). The overall cell performance was a balance between improved anode kinetics and greater methanol crossover causing greater cathode losses, when methanol feed concentration was increased. The crossover influence is more evident with air due to the lower O_2 concentration as discussed earlier. Thus for practical DMFC operation with air, the use of a Pd cathode catalyst would appear to be suitable for higher methanol concentration feeds ($>5 \text{ M}$) when reasonable cell voltages are required of $>300 \text{ mV}$.

Figure 7 shows chronoamperometry measurements of DMFC with Pd/C or Pt/C as cathode catalyst at 20°C and 5 M methanol with oxygen over 15 hours operation. Both MEAs showed very similar behavior in the studied 15 hrs period. Sharp drop was observed in the first 20 mins in both Pt- and Pd-based cathode MEAs. After one hour of operation, very slow decline was observed on both MEAs with rate of 0.19 and $0.3 \text{ mA}\cdot\text{cm}^{-2}\cdot\text{hr}^{-1}$ for MEAs with Pd and Pt cathodes, respectively. This suggests that Palladium is a stable substitute to Platinum as cathode materials in DMFCs.

3.2. *Cathode Polarizations.* The amount of methanol crossover from anode to cathode through the electrolyte

membrane (methanol cross-over) in a DMFC increases with increasing methanol concentration and temperature. The presence of methanol in the cathode decreases its performance by hindering the access of the oxygen molecules to the catalyst sites and, in some cases, by the ‘‘mixed potential’’ effect [26]. On the other hand, methanol oxidation reaction can improve with increasing methanol concentration and temperature. Therefore, the overall cell performance is a balance of the two factors. In this section, the influence of the methanol concentration on the cathode performance was studied at 60°C .

Methanol crossover at 60°C and 1 M MeOH was measured using an electrochemical technique. During the measurement, nitrogen was introduced into the cathode side (platinum case) and a positive voltage was applied using a power supply. The reaction occurring at the cathode is the oxidation of methanol that crosses through the membrane. When the applied voltage is high enough to quickly oxidize all the methanol diffusing to the cathode side, a limiting current is achieved. This limiting current represents approximately the rate of methanol crossover at open circuit [27]. The obtained value was ca. $63 \text{ mA}\cdot\text{cm}^{-2}$ with 1 M MeOH feed at the anode. Considering exchange current density at room temperature for the oxygen reduction reaction (ORR) on platinum electrode is $1.4 \times 10^{-10} \text{ A}\cdot\text{cm}^{-2}_{\text{ECSA}}$ [11] and activation energy of ca. $26 \text{ kJ}\cdot\text{mol}^{-1}$ [20], this estimates ORR exchange current density on Pt/C at 60°C to be $4.22 \times 10^{-10} \text{ A}\cdot\text{cm}^{-2}_{\text{ECSA}}$, and from Table 1 the ECSA for 20% Pt/C is recorded to be $55.3 \text{ m}^2\cdot\text{g}^{-1}$. The potential loss estimated due to methanol cross-over of $63 \text{ mA}\cdot\text{cm}^{-2}$ (considering cathode loading of $2 \text{ mg}\cdot\text{cm}^{-2}$) can be estimated to ca. 300 mV using the following simplified equation [28]:

$$\eta_{\text{cross-over}} = \frac{-RT}{\alpha F} \ln \left[\frac{i_{\text{cross-over}}}{2i_{0,c}} + \sqrt{1 + \left(\frac{i_{\text{cross-over}}}{2i_{0,c}} \right)^2} \right], \quad (3)$$

where α is the transfer coefficient and i_0 is the exchange current density.

TABLE 4: Current densities at 0.4 V, cell voltage at $5 \text{ mA} \cdot \text{cm}^{-2}$, open circuit potential and peak power densities for a direct methanol fuel cell with 5 M methanol solution fed to the anode at 20, 40, and 60°C.

Cathode catalyst	Temperature (°C)	Cathode fed	Voltage at $5 \text{ mA} \cdot \text{cm}^{-2}$ (mV)	Open circuit potential (mV)	Current density at 0.4 V ($\text{mA} \cdot \text{cm}^{-2}$)	Peak power density (mW cm^{-2})
Pd/C	20	Air	498	685	14	11.5
Pt/C-Etek	20	Air	497	641	14.5	14.9
Pd/C	20	O ₂	510	704	28.7	26.5
Pt/C-Etek	20	O ₂	562	700	26.2	20.3
Pd/C	40	Air	505	631	18	15.3
Pt/C-Etek	40	Air	514	631	24	26.6
Pd/C	40	O ₂	540	678	35.1	22
Pt/C-Etek	40	O ₂	566	686	36.3	26
Pd/C	60	Air	507	616	25.2	20.6
Pt/C-Etek	60	Air	508	607	19.6	19
Pd/C	60	O ₂	559	660	43.8	30
Pt/C-Etek	60	O ₂	588	702	65.1	40.5

TABLE 5: Current densities at 0.4 V, cell voltage at $5 \text{ mA} \cdot \text{cm}^{-2}$, open circuit potential and peak power densities for a direct methanol fuel cell with 3, 5, and 7 M methanol solution fed to the anode at 60°C.

Cathode catalyst	Methanol concentration (mol L^{-1})	Cathode fed	Voltage at $5 \text{ mA} \cdot \text{cm}^{-2}$ (mV)	Open circuit potential (mV)	Current density at 0.4 V ($\text{mA} \cdot \text{cm}^{-2}$)	Peak power density (mW cm^{-2})
Pd/C	3	Air	503	654	14.7	19.1
Pt/C-Etek	3	Air	519	615	26.4	25.7
Pd/C	3	O ₂	566	690	40	26
Pt/C-Etek	3	O ₂	590	699	59.4	37.8
Pd/C	5	Air	507	616	25.2	20.6
Pt/C-Etek	5	Air	508	607	19.6	19
Pd/C	5	O ₂	559	660	43.8	30
Pt/C-Etek	5	O ₂	588	702	65.1	40.5
Pd/C	7	Air	503	600	24.9	17.2
Pt/C-Etek	7	Air	400	472	5.0	12.8
Pd/C	7	O ₂	558	665	44.6	30.9
Pt/C-Etek	7	O ₂	556	671	50.1	38.5

TABLE 6: Comparison of Pd catalysts performance with published data.

Catalyst	Output	I/ECSA	Operating conditions	Reference
Pd/C + Pt/C	$20 \text{ mA} \cdot \text{cm}^{-2}$	$31 \mu\text{A cm}^{-2}$	0.4 V, 30°C, 5 M methanol, 0.5 L/min air, $2 \text{ mg} \cdot \text{cm}^{-2}$ Pt + $1 \text{ mg} \cdot \text{cm}^{-2}$ Pd	[24]
Pt/C	$9 \text{ mA} \cdot \text{cm}^{-2}$	$7 \mu\text{A cm}^{-2}$	0.4 V, 30°C, 5 M methanol, 0.5 L/min air, $4 \text{ mg} \cdot \text{cm}^{-2}$ Pt	[24]
Pd ₃ Co/C	$20 \text{ mA} \cdot \text{cm}^{-2}$	$65 \mu\text{A cm}^{-2}$	0.4 V, 60°C, 0.5 M methanol, oxygen, $0.2 \text{ mg} \cdot \text{cm}^{-2}$ Pd ₃ Co	[22]
Pd ₃ Pt/C	$225 \text{ mA} \cdot \text{cm}^{-2}$	$400 \mu\text{A cm}^{-2}$	0.4 V, 75°C, 1 M methanol, oxygen 0.2 MPa, $1 \text{ mg} \cdot \text{cm}^{-2}$ Pd ₃ Pt	[25]
Pd/C	$8 \text{ mA} \cdot \text{cm}^{-2}$	$27 \mu\text{A cm}^{-2}$	0.4 V, 40°C, 1 M methanol, 0.3 L/min air, $2 \text{ mg} \cdot \text{cm}^{-2}$ Pd	This work
Pt/C	$17 \text{ mA} \cdot \text{cm}^{-2}$	$15 \mu\text{A cm}^{-2}$	0.4 V, 60°C, 1 M methanol, 0.3 L/min air, $2 \text{ mg} \cdot \text{cm}^{-2}$ Pt	This work
Pd/C	$13 \text{ mA} \cdot \text{cm}^{-2}$	$43 \mu\text{A cm}^{-2}$	0.4 V, 60°C, 1 M methanol, 0.3 L/min air, $2 \text{ mg} \cdot \text{cm}^{-2}$ Pd	This work
Pt/C	$27 \text{ mA} \cdot \text{cm}^{-2}$	$25 \mu\text{A cm}^{-2}$	0.4 V, 60°C, 1 M methanol, 0.3 L/min air, $2 \text{ mg} \cdot \text{cm}^{-2}$ Pt	This work
Pd/C	$18 \text{ mA} \cdot \text{cm}^{-2}$	$60 \mu\text{A cm}^{-2}$	0.4 V, 40°C, 5 M methanol, 0.3 L/min air, $2 \text{ mg} \cdot \text{cm}^{-2}$ Pd	This work
Pt/C	$24 \text{ mA} \cdot \text{cm}^{-2}$	$22 \mu\text{A cm}^{-2}$	0.4 V, 40°C, 5 M methanol, 0.3 L/min air, $2 \text{ mg} \cdot \text{cm}^{-2}$ Pt	This work
Pd/C	$25 \text{ mA} \cdot \text{cm}^{-2}$	$83 \mu\text{A cm}^{-2}$	0.4 V, 60°C, 5 M methanol, 0.3 L/min air, $2 \text{ mg} \cdot \text{cm}^{-2}$ Pd	This work
Pt/C	$20 \text{ mA} \cdot \text{cm}^{-2}$	$18 \mu\text{A cm}^{-2}$	0.4 V, 60°C, 5 M methanol, 0.3 L/min air, $2 \text{ mg} \cdot \text{cm}^{-2}$ Pt	This work

Cathode polarization curves were obtained by adding cell (operating with oxygen) and anode potential-current curves [29]. To obtain anode polarization curves, H₂ was passed through the cathode, to act as a Normal Hydrogen Electrode (NHE) [26]. The cathode data were essentially IR-free since the anode data inherently included the IR losses (membrane and catalyst layer). Figure 8 shows the effect of methanol concentration on the anode polarization curves at 60°C. Current densities increased with increasing methanol concentration, where for example, at 400 mV for 1, 3, 5, and 7 M methanol concentration values were 23.2, 26.1, 30.2, and 38.5 mA·cm⁻², respectively.

These anode polarization curves demonstrated how anode performance increased with fuel concentration. However, this does not apply to the overall cell performance mainly due to the effect of methanol crossover. There is an optimum methanol concentration at which the cell would exhibit its maximum performance. This optimum methanol concentration depends on various parameters, including temperature and cathode catalyst. Ko et al. built a dynamic model to study the influence of different parameters on cell performance, and according to their model, the optimal methanol concentration using Pt/C in the cathode and at 60°C was ca. 1 M [30]. Since the activity of Pd/C towards the methanol oxidation reaction is lower than that of Pt/C, the optimal methanol concentration when using Pd/C as cathode material is expected to be higher.

Figure 6 shows cathode polarization curves for the Pt MEA at different methanol concentration. Data is compared to polarization curves, in the corresponding current range, obtained from a hydrogen PEM fuel cell. Data for the hydrogen-fed PEMFC were obtained using from a single low temperature H₂/O₂ PEMFC with a Nafion 112 membrane (cathode data include H₂ cross-over effects) [11]. Cathode potentials with 1, 3, and 5 M methanol solution rose with increasing current density; this behavior is attributed to the improvement of cell performance with increased oxidation of methanol at the anode and with the initial oxidation of the methanol present in the cathode (methanol crossed-over is oxidized when the cell is polarized), as discussed in the work of Gurau and smotkin [23]. Using 7 M methanol, there was a sharp decrease in the rest potential ($i = 0$), of approximately 150 mV, compared to 5 M, which was maintained over most of the cathode potential range, and confirmed the poorer cathode performance with increased methanol concentration.

DMFC data in Figure 9 is compared with data from a hydrogen fuel cell. At low current densities (<10 mA·cm⁻²), there was a difference of ca. 200 mV between the DMFC (using methanol 1, 3, and 5 M) and the hydrogen fuel cell with the same metal loading. At larger current densities, 10 mA·cm⁻², this difference decreased up to ca. 100 mV for 1, 3, and 5 M methanol solution. This illustrates that when the cell is polarized, the methanol present in the cathode was consumed and the behavior of both cathodes became closer. Also, as current was drawn the crossover of methanol fell and thus the cathode partially recovered.

Since the Pt loading in the cathode of the DMFC was approximately 3.3 times larger than the loading in the

hydrogen fuel cell, an estimation of the performance of the hydrogen fuel cell with higher loading was made to provide the data in Figure 9 (and following data).

From Tafel equation, we can write

$$\begin{aligned}\eta_1 &= \frac{RT}{\alpha nF} \ln i - \frac{RT}{\alpha nF} \ln i_0, \\ \eta_2 &= \frac{RT}{\alpha nF} \ln i - \frac{RT}{\alpha nF} \ln i_0^*,\end{aligned}\quad (4)$$

where i is current density, η_1 and η_2 are cell overpotentials, and i_0 and i_0^* are apparent exchange current densities with cathode metal loadings of 2.0 and 0.6 mg·cm⁻², respectively. Since apparent exchange current density is proportional to the electrochemically active surface area and this is proportional to the catalyst loading $3.3 \times i_0^* = i_0$, subtracting (4):

$$\eta_2 - \eta_1 = \frac{RT}{\alpha nF} \ln 3.3. \quad (5)$$

Solving (5) the difference $\eta_2 - \eta_1$ equals 69 mV. This amount was added to the potential on the data corresponding to a metal loading 0.6 mg·cm⁻² to obtain the estimated curve for a loading 2.0 mg·cm⁻².

Figure 10 compares cathode polarization curves for the Pd MEA at different methanol concentration with data obtained from a hydrogen PEM fuel cell. It is clear that whilst Pd cathode data with a methanol-free cathode exhibited lower rest potential (or onset) than Pt by 120 mV (ca. 1000 versus 880 mV), the Pd cathode potential losses due to the mixed potential caused by the methanol crossover were significantly lower. For example, with 5 M it was approximately 100 mV for Pd compared to 200 for Pt; therefore, the overall difference between the two cathodes (with air operation) using 5 M methanol was small. At higher concentrations, Pd offers an advantage over Pt. The effect of crossover would be even more severe at lower cathode loading because the current generated from oxygen reduction would be lower and therefore Pd would surpass Pd at even lower methanol concentrations.

Experimental results agreed with studies published by McGrath [24], where it was shown how the partial substitution of Pt by Pd in the cathode led to higher cell performance at high methanol concentrations, even with lower total metal loading. Comparison data from this study are compared with the limited published data on the use of Pd-based cathodes in Table 6. The values for ECSA used in the calculations were obtained from the relevant source [22, 24, 25] while that for commercial Platinum was obtained from [28].

3.3. Effect of Temperature on Fuel Cell Performance. Anode and cathode polarization curves at different temperatures for a fuel cell with PtRu/C from E-tek in the anode and fed with 5 M methanol solution are shown in Figure 11. The increase of temperature increased the anode performance by increasing the kinetics of the methanol oxidation reaction. Anode currents at 400 mV at 20, 40, and 60°C were 10.2, 17.8, and 30.2 mA·cm⁻², respectively.

However, although anode performance improved with an increase in temperature; an increase in temperature also increased methanol crossover to the cathode due to faster diffusion. The dependence of methanol permeability on temperature through Nafion has been reported to follow Arrhenius behavior: for Nafion 117 at 20, 40, and 60°C values were ca. 14×10^{-7} , 22×10^{-7} , and $34 \times 10^{-7} \text{ cm}^2 \text{ s}^{-1}$, respectively [31]. Thus a greater crossover rate when the temperature was increased from 40 to 60°C was the main cause of the lack of significant increase in cell performance with temperature at low current densities.

For the Pt MEA fed with 5 M methanol solution, the highest cathode potential at low current densities ($10 \text{ mA} \cdot \text{cm}^{-2}$) was obtained at 20°C, ca. 830 mV, and remained constant up to $100 \text{ mA} \cdot \text{cm}^{-2}$. At higher current densities, the reverse trend was seen, which confirmed the effect discussed above between a balance between methanol crossover effect and activation kinetics when temperature was increased. Data was compared with data from a hydrogen fuel cell, all Pt cathode polarizations using 5 M methanol were at least 200 mV lower than that predicted for a hydrogen fuel cell with the same loading.

Figure 11(c) shows cathode polarization curves for the Pd MEA fed with 5 M methanol solution at 20, 40, and 60°C. The trend with increasing temperature was similar to that with Pt in the low current density region, the cathode potential decreased slightly with the temperature. However, the difference with hydrogen fuel cell data is less than 60 mV at any operating temperature. At 60°C with air operation (suitable operating conditions for a DMFC) and at low current densities, Pd cathodes match the performance of a Pt cathode with the same metal loading when 5 M methanol is fed to the anode.

4. Conclusions

Pd/C was tested as a cathode catalyst in a direct methanol fuel cell and its performance was compared to a commercial Pt/C.

Anode potential versus current density curves showed that anode performance increased with increasing temperature and methanol concentration. This behaviour was not always reflected in the overall cell performance due to methanol crossover to the cathode. The effect of methanol crossover was more severe for the Pt cathode due to its higher activity towards the methanol oxidation reaction.

Cathode potentials in the DMFC were affected by methanol crossover in that relatively high polarization was experienced at low current densities which tended to decrease at higher current densities. Despite its relatively lower electrochemical surface area, palladium performed better than Pt as a cathode catalyst at high methanol concentrations. Current densities at 400 mV obtained with the palladium MEA were higher than those with platinum at 60°C with methanol concentrations of 5 M or higher. This data indicated that Pd could be an adequate substitute to Pt due to its lower price. Moreover, since the effect of crossover would be more severe for Pt at lower cathode loadings

(lower ORR current), the performance of a Pd cathode could be higher than that of a Pt cathode even lower than 5 M (equal performance at low current densities with $2 \text{ mg} \cdot \text{cm}^{-1}$ cathode loading).

Acknowledgment

EPSRC supported this work through a studentship to G. F. Álvarez from the SUPERGEN Fuel cell consortium award.

References

- [1] R. W. Reeve, P. A. Christensen, A. J. Dickinson, A. Hamnett, and K. Scott, "Methanol-tolerant oxygen reduction catalysts based on transition metal sulfides and their application to the study of methanol permeation," *Electrochimica Acta*, vol. 45, no. 25-26, pp. 4237–4250, 2000.
- [2] H. Cheng, W. Yuan, and K. Scott, "The influence of a new fabrication procedure on the catalytic activity of ruthenium-selenium catalysts," *Electrochimica Acta*, vol. 52, no. 2, pp. 466–473, 2006.
- [3] M. Hilgendorff, K. Diesner, H. Schulenburg, P. Bogdanoff, M. Bron, and S. Fiechter, "Preparation strategies towards selective Ru-based oxygen reduction catalysts for direct methanol fuel cells," *Journal of New Materials for Electrochemical Systems*, vol. 5, no. 2, pp. 71–81, 2002.
- [4] H. Schulenburg, M. Hilgendorff, I. Dorbandt et al., "Oxygen reduction at carbon supported ruthenium-selenium catalysts: selenium as promoter and stabilizer of catalytic activity," *Journal of Power Sources*, vol. 155, no. 1, pp. 47–51, 2006.
- [5] K. Kinoshita and Electrochemical Society, *Electrochemical Oxygen Technology*, vol. 431 of *The Electrochemical Society*, John Wiley & Sons, New York, NY, USA, 1992.
- [6] K. Lee, O. Savadogo, A. Ishihara, S. Mitsushima, N. Kamiya, and K. I. Ota, "Methanol-tolerant oxygen reduction electrocatalysts based on Pd-3D transition metal alloys for direct methanol fuel cells," *Journal of the Electrochemical Society*, vol. 153, no. 1, pp. A20–A24, 2006.
- [7] H. Li, Q. Xin, W. Li et al., "An improved palladium-based DMFCs cathode catalyst," *Chemical Communications*, no. 23, pp. 2776–2777, 2004.
- [8] JI. B. Joo, Y. J. Kim, W. Kim et al., "Methanol-tolerant PdPt/C alloy catalyst for oxygen electro-reduction reaction," *Korean Journal of Chemical Engineering*, vol. 25, no. 4, pp. 770–774, 2008.
- [9] IN. T. Kim, H. K. Lee, and J. Shim, "Synthesis and characterization of Pt-Pd catalysts for methanol oxidation and oxygen reduction," *Journal of Nanoscience and Nanotechnology*, vol. 8, no. 10, pp. 5302–5305, 2008.
- [10] J. Lin, A. Trivisonno, R. Wycisk, and P. N. Pintauro, "Optimized DMFC performance comparison for modified and unmodified nafion membranes," in *Proceedings of the 210th Meeting of The Electrochemical Society (ECS '06)*, pp. 63–71, November 2006.
- [11] G. F. Alvarez, K. Scott, M. Mamlouk, and S. M. S. Kumar, "Preparation and characterisation of carbon-supported palladium nano-particles for oxygen reduction in low and high temperature PEM fuel cells," submitted to *Journal of Applied Electrochemistry*.
- [12] M. W. Breiter, "Dissolution and adsorption of hydrogen at smooth Pd wires at potentials of the alpha phase in sulfuric

- acid solution,” *Journal of Electroanalytical Chemistry*, vol. 81, no. 2, pp. 275–284, 1977.
- [13] T. Mallát, E. Polyánszky, and J. Petró, “Electrochemical study of palladium powder catalysts,” *Journal of Catalysis*, vol. 44, no. 3, pp. 345–351, 1976.
- [14] L. Zhang, K. Lee, and J. Zhang, “Effect of synthetic reducing agents on morphology and ORR activity of carbon-supported nano-Pd-Co alloy electrocatalysts,” *Electrochimica Acta*, vol. 52, no. 28, pp. 7964–7971, 2007.
- [15] A. Guha, W. Lu, T. A. Zawodzinski, and D. A. Schiraldi, “Surface-modified carbons as platinum catalyst support for PEM fuel cells,” *Carbon*, vol. 45, no. 7, pp. 1506–1517, 2007.
- [16] C. Wu, H. Zhang, and B. Yi, “Hydrogen generation from catalytic hydrolysis of sodium borohydride for proton exchange membrane fuel cells,” *Catalysis Today*, vol. 93–95, pp. 477–483, 2004.
- [17] B. D. Cullity, *Elements of X-Ray Diffraction*, Addison-Wesley, Reading, Mass, USA, 1978.
- [18] X. Li, Q. Huang, Z. Zou, B. Xia, and H. Yang, “Low temperature preparation of carbon-supported Pd-Co alloy electrocatalysts for methanol-tolerant oxygen reduction reaction,” *Electrochimica Acta*, vol. 53, no. 22, pp. 6662–6667, 2008.
- [19] W. E. Mustain and J. Prakash, “Kinetics and mechanism for the oxygen reduction reaction on polycrystalline cobalt-palladium electrocatalysts in acid media,” *Journal of Power Sources*, vol. 170, no. 1, pp. 28–37, 2007.
- [20] U. A. Paulus, T. J. Schmidt, H. A. Gasteiger, and R. J. Behm, “Oxygen reduction on a high-surface area Pt/Vulcan carbon catalyst: a thin-film rotating ring-disk electrode study,” *Journal of Electroanalytical Chemistry*, vol. 495, no. 2, pp. 134–145, 2001.
- [21] F. Kadirgan, B. Beden, J. M. Leger, and C. Lamy, “Synergistic effect in the electrocatalytic oxidation of methanol on platinum+palladium alloy electrodes,” *Journal of Electroanalytical Chemistry*, vol. 125, no. 1, pp. 89–103, 1981.
- [22] W. E. Mustain, K. Kepler, and J. Prakash, “CoPd oxygen reduction electrocatalysts for polymer electrolyte membrane and direct methanol fuel cells,” *Electrochimica Acta*, vol. 52, no. 5, pp. 2102–2108, 2007.
- [23] B. Gurau and E. S. Smotkin, “Methanol crossover in direct methanol fuel cells: a link between power and energy density,” *Journal of Power Sources*, vol. 112, no. 2, pp. 339–352, 2002.
- [24] K. McGrath, “High Concentration Direct Methanol Fuel Cell Using QSI-Nano® Pd,” Energy Research Laboratory, QuantumSphere Inc., 2008.
- [25] H. Li, Q. Xin, W. Li et al., “An improved palladium-based DMFCs cathode catalyst,” *Chemical Communications*, no. 23, pp. 2776–2777, 2004.
- [26] H. Liu and J. Zhang, *Electrocatalysis of Direct Methanol Fuel Cells*, Wiley-VCH, Weinheim, Germany, 2009.
- [27] Z. Qi and A. Kaufman, “Open circuit voltage and methanol crossover in DMFCs,” *Journal of Power Sources*, vol. 110, no. 1, pp. 177–185, 2002.
- [28] M. Mamlouk, T. Sousa, and K. Scott, “A high temperature polymer electrolyte membrane fuel cell model for reformat gas,” *International Journal of Electrochemistry*, vol. 2011, Article ID 520473, 18 pages, 2011.
- [29] W. Vielstich, H. Gasteiger, and A. Lamm, *Handbook of Fuel Cells: Fundamentals, Technology and Applications*, vol. 4, John Wiley & Sons, Chichester, UK, 2003.
- [30] D. Ko, M. Lee, W. H. Jang, and U. Krewer, “Non-isothermal dynamic modelling and optimization of a direct methanol fuel cell,” *Journal of Power Sources*, vol. 180, no. 1, pp. 71–83, 2008.
- [31] V. Tricoli, N. Carretta, and M. Bartolozzi, “Comparative investigation of proton and methanol transport in fluorinated ionomeric membranes,” *Journal of the Electrochemical Society*, vol. 147, no. 4, pp. 1286–1290, 2000.



Hindawi

Submit your manuscripts at
<http://www.hindawi.com>

